Global nonambipolar flow: Plasma confinement where all electrons are lost to one boundary and all positive ions to another boundary

S. D. Baalrud, N. Hershkowitz, and B. Longmier
Engineering Physics, University of Wisconsin-Madison, Madison, Wisconsin 53706

(Received 18 January 2007; accepted 14 March 2007; published online 30 April 2007)

A new mode of plasma confinement is demonstrated in which essentially all positive ions leave the plasma to only one boundary while essentially all electrons are lost to a different boundary. Sheaths near the plasma boundaries are entirely responsible for this global nonambipolar flow. The bulk plasma remains quasineutral and unperturbed even when all electrons are lost to only one, physically small, location. A necessary condition for global nonambipolar flow depends on the ratio of electron collection area to ion collection area. The plasma electron temperature is significantly higher in the global nonambipolar mode than in the typical ambipolar mode due to a relative increase in confinement of high-energy electrons and a relative decrease in confinement of low-energy electrons. © *2007 American Institute of Physics*. [DOI: 10.1063/1.2722262]

I. INTRODUCTION

Sheaths are non-neutral regions found near plasma boundaries that act to balance the electrons and ions lost globally from a plasma. The characteristics of sheaths are well known. There are two varieties: electron and ion. Ion sheaths act to reflect part of the incident electron current, and electron sheaths the ion current. In all devices in which the details of electron loss have been studied, the majority of electrons were lost through ion sheaths. Electron sheaths have sometimes been present, but have never collected a substantial fraction of the electron current lost globally from the plasma.[1–4] In this paper, we show that it is possible to collect all of the electron current leaving a plasma through an electron sheath without perturbing the plasma itself. We define this new mode of plasma confinement as global nonambipolar flow. Electron sources are used in a wide variety of applications: plasma processing,[5] plasma generation,[6] chemical vapor deposition,[7] ion thruster neutralization,[8] etc. Global nonambipolar flow is the most efficient way to extract electrons and it can be utilized in electron source design.[9]

Langmuir was the first to suggest that the sheath near a positive electrode could be either an ion or electron sheath depending on its surface area.[10] It is generally recognized that electron sheaths can occur near small positively biased objects inserted into plasmas, but "small" has never been defined. We show that the sheath near an electron collecting boundary is somewhat more complicated than Langmuir envisioned; it can either be a monotonic ion sheath, a monotonic electron sheath, or a double sheath. We establish a necessary condition that the ratio of the electron collecting area to ion collecting area must satisfy for each of these sheath solutions and we show that global nonambipolar flow can be achieved when a double sheath is present.

II. GLOBAL FLOW AND SHEATH MODELS

We consider an unmagnetized, low-temperature, weakly collisonal plasma with collisionless sheaths where the electron temperature, T_e, is much greater than the positive ion temperature, T_i, and all ions are singly ionized. Collisionless sheath thickness can be described by the Child-Langmuir law, $s \propto \Delta V^{3/4}$, when $\exp(-e\Delta V/T_e) \ll 1$, where ΔV is the potential drop across the sheath and T_e is measured in electron volts.[11] Furthermore, we assume that the plasma boundaries can be approximated as planar and that the plasma ions and electrons can be described by separate Maxwellian distribution functions in velocity space. The plasma potential is determined by balancing the positive ion and electron currents lost globally from the plasma.

If the plasma is confined by a single boundary, then global ambipolar flow ensues where the average ion and electron flux equate at each macroscopic location of the boundary,[11]

$$\Gamma_e = \frac{1}{4} e n_0 \bar{v}_e \exp\left(-\frac{e\Delta\varphi}{T_e}\right) = \Gamma_{i,B} = 0.6 e n_0 c_s, \tag{1}$$

where $\bar{v}_e = \sqrt{8T_e/\pi m_e}$ is the mean electron speed at the sheath edge, $c_s \equiv \sqrt{T_e/M_i}$ is the ion sound speed, m_e is the electron mass, M_i is the positive ion mass, and n_0 denotes the ion and electron density in the quasineutral bulk plasma. The factor of 0.6 multiplying the ion flux is due to reduction in density through the ion presheath, which, according to Bohm's criterion, must have a potential drop $\Delta\varphi_{\mathrm{ps}} \geq T_e/2e$.[12] Assuming the minimum presheath potential drop, Boltzmann's relation gives $n_s \cong 0.6 n_0$ for the ion density at the sheath edge where ion fluid speed is c_s. $\Delta\varphi$ includes both the presheath and sheath potential drops. Assigning the wall potential to be the reference, $\Delta\varphi = V_p - V_w = V_p$, the bulk plasma potential is

$$V_p = -\frac{T_e}{e}\ln(\mu), \tag{2}$$

where $\mu \equiv \sqrt{2.3 m_e/M_i}$.

Ambipolar loss occurs at a surface when ion and electron flux equate at that surface. For example, insulators and electrically floating conductors experience ambipolar loss. If ambipolar loss occurs at every boundary of the plasma, we say that global ambipolar flow ensues. However, if the

plasma is contained by multiple conducting boundaries at different potentials, electron and ion flux will not equate at each boundary. If a boundary collects only electrons or ions, for example a small biased probe, we say that nonambipolar loss occurs at that surface. When all of the plasma boundaries can be split into only two categories—those that collect only electrons and those that collect only ions—we say that global nonambipolar flow ensues. The simplest demonstration is for two boundaries: one collecting only electrons and one collecting only ions. In this case, global nonambipolar flow can be established through a combination of electron and ion sheaths created by simply biasing an appropriately sized electron collecting boundary much more positive than the ion collecting boundary.

To demonstrate this, consider placing a planar disk-shaped auxiliary electrode (AE) of surface area A_{AE} biased much more positive than the confining chamber wall ($V_{\mathrm{AE}} \gg 0$), of area A_w, into a uniform discharge. The global current balance, which depends on the areas available for electron and ion loss, will determine the form of the sheath near AE and the resulting global flow scenario. There are three possible solutions that depend on the ratio of surface areas A_{AE}/A_w.

If monotonic ion sheaths are present near both boundaries, ions are lost at the Bohm current to each boundary, $I_i = \Gamma_{i,B}(A_{\mathrm{AE}}+A_w)$, and electrons are lost through the ion sheaths at each boundary, $I_e = \Gamma_{e,\mathrm{th}}[A_{\mathrm{AE}} \exp(-e\Delta\varphi_{\mathrm{AE}}/T_e) + A_w \exp(-eV_p/T_e)]$, where $\Gamma_{e,\mathrm{th}} = en_0\bar{v}_e/4$, and $\Delta\varphi_{\mathrm{AE}} = V_p - V_{\mathrm{AE}} \geq T_e/2e$ from Bohm's criterion for a stable ion sheath.[12] Balancing the two currents and solving for the plasma potential gives

$$V_p = -\frac{T_e}{e}\ln\left[\frac{A_w + A_{\mathrm{AE}}}{A_w}\mu - \frac{A_{\mathrm{AE}}}{A_w}\exp\left(-\frac{e\Delta\varphi_{\mathrm{AE}}}{T_e}\right)\right]. \quad (3)$$

Applying the assumption that the AE is biased much more positive than the chamber wall, $V_p \gg T_e$, a condition for the AE area needed for a stable monotonic ion sheath follows directly from (3)

$$\frac{A_{\mathrm{AE}}}{A_w} \geq \left(\frac{0.6}{\mu} - 1\right)^{-1} \cong 1.7\mu. \quad (4)$$

If a monotonic electron sheath is present near the AE when it is biased at least a few volts more positive than the plasma, essentially no ions are lost to the AE because $T_i \ll \Delta\varphi_{\mathrm{AE}}$. Ions are lost only to the chamber wall at the Bohm current, $I_i = \Gamma_{i,B}A_w$. Electrons are lost to both boundaries, so $I_e = \Gamma_{e,\mathrm{th}}[A_{\mathrm{AE}} + A_w \exp(-eV_p/T_e)]$. Equating electron and ion losses then gives

$$V_p = -\frac{T_e}{e}\ln\left(\mu - \frac{A_{\mathrm{AE}}}{A_w}\right), \quad (5)$$

which requires

$$A_{\mathrm{AE}}/A_w < \mu \quad (6)$$

as a necessary condition for a monotonic electron sheath to exist near the AE.

When $\mu < A_{\mathrm{AE}}/A_w < [(0.6/\mu)-1]^{-1}$, neither a monotonic electron sheath nor a monotonic ion sheath can exist near the AE. Instead, a double sheath forms to preserve quasineutrality and balance the total electron and ion currents lost from the bulk plasma. The double sheath potential profile looks like a dip, or a combination of electron and ion sheaths, in which $V_{\mathrm{AE}} > V_p > V_D$, where V_D is the potential at the dip minimum. Defining $\Delta\varphi_D \equiv V_p - V_D$, and assuming again that $e(V_{\mathrm{AE}} - V_p)/T_i \gg 1$, no ions are lost to the AE, and the plasma potential is again solved by balancing electron and ion currents

$$V_p = -\frac{T_e}{e}\ln\left[\mu - \frac{A_{\mathrm{AE}}}{A_w}\exp\left(-\frac{e\Delta\varphi_D}{T_e}\right)\right]. \quad (7)$$

With A_{AE}/A_w satisfying the above inequality, and $eV_p/T_e \gg 1$, electrons are only lost to the AE and ions are only lost to the chamber wall. This is the global nonambipolar flow regime because here all electrons are collected by the AE, which is biased more positively than the plasma potential, while all positive ions are collected by the chamber wall, which is biased more negative than the plasma potential. Under these conditions, the dip potential drop is

$$\Delta\varphi_D = -\frac{T_e}{e}\ln\left(\frac{A_w}{A_{\mathrm{AE}}}\mu\right). \quad (8)$$

Equation (8) shows that in global nonambipolar mode, $V_p - V_D$ does not depend on V_{AE}. The Child-Langmuir law for collisionless sheaths, $s \propto \Delta V^{3/4}$, suggests that the thickness of the ion sheath portion of the double sheath, s, is constant in this regime. Consequently, the thickness of the electron portion of the double sheath, also given by a Child-Langmuir law,

$$d = \frac{\sqrt{2}}{3}\lambda_{D,d}\left(\frac{2e(V_{\mathrm{AE}} - V_D)}{T_e}\right)^{3/4}, \quad (9)$$

must also remain invariant with changing AE bias. If the AE potential rose or fell at a different rate than the potential of the dip minimum, the electron sheath thickness d would contract or expand, both in the axial and radial directions. Contraction or expansion in the radial direction would alter the effective cross-sectional area of the AE. Since this would change the total electron current lost from the plasma, which is all lost to the AE in a global nonambipolar mode, d must remain invariant to preserve global current balance. Because the ion and electron portions of the double sheath do not depend on V_{AE}, $V_{\mathrm{AE}} - V_p$ also remains invariant, i.e., the plasma potential "locks" with the AE potential in the global nonambipolar regime.

The electron temperature is strongly correlated with the global flow scenario in the plasma. In global ambipolar flow, only electrons with energy greater than the plasma potential, given in Eq. (1), can escape the plasma. Slower electrons with less energy are confined by the ion sheath near each boundary. However, when global nonambipolar flow occurs, essentially all electrons are reflected from the high-voltage ion sheath at the chamber wall while essentially all of the electrons incident on the AE are lost to it independent of electron kinetic energy. The electron energy required to be

lost to the AE is that necessary to overcome the potential dip given in Eq. (8). The required electron energy is essentially zero when $A_{AE} \cong \mu A_w$.

The loss rate of a particle is proportional to the product of its speed and the physical boundary area available for it to be lost to. So a result of global nonambipolar flow is increased confinement of high-energy electrons (with energy $>eV_p$), relative to global ambipolar flow, since high-energy electrons are lost only to the AE instead of either the AE or the chamber wall. A second result is decreased confinement of low-energy electrons (with energy $<eV_p$) since in global nonambipolar flow these electrons are lost to the AE, whereas in global ambipolar flow they are lost nowhere. Here V_p refers to the plasma potential in global ambipolar flow. The combination of increased confinement of high-energy electrons and decreased confinement of low-energy electrons in global nonambipolar flow results in a significantly larger electron temperature than in global ambipolar flow.

III. DESCRIPTION OF EXPERIMENT

Our experiments were conducted in a cylindrical MacKenzie bucket[13] of diameter 60 cm and length 70 cm, Fig. 1. Twelve rows of permanent magnets were placed symmetrically around the circumference, oriented so that the magnetic dipole alignment alternated between successive magnet rows, and the end walls were not magnetized.[14] The multidipole magnets helped create a uniform discharge in the radial direction by reducing plasma diffusion to the radial boundary. The bulk plasma was essentially not magnetized. Peak magnetic field along the chamber axis was less than 2 G. Near the chamber side wall the peak magnetic field was approximately 1 kG, at locations near the permanent magnets, and the minimum field was less than 10 G, at locations between the magnets.

Argon plasma was generated from a 0.5 A current of electrons emitted from heated, thoriated tungsten filaments biased at −60 V with respect to the grounded aluminum chamber wall. The plasma acted as a virtual anode for the filament electrons, which were accelerated from the negative filament bias to the plasma potential. The area of the filaments and filament supports was approximately 10 cm^2. The base chamber pressure was less than 1×10^{-3} mTorr and operating neutral pressures varied from 0.7 to 1.0 mTorr. A dc power source was used to bias the thin (~2 mm) aluminum disk (AE) that was held in the middle of the multidipole chamber by a 0.6 cm diameter copper rod that was electrically insulated from the plasma with a thin fiberglass sleeve. The AEs used were two-sided, and their area was varied by choosing AEs with different radii.

The bulk plasma potential, electron density, and electron temperature were measured using an 8 mm diameter planar Langmuir probe located 15 cm from the AE and along the chamber axis. The plane of the two-sided Langmuir probe was oriented parallel to the plane of the AE and the 15 cm distance was chosen to ensure that the Langmuir probe measured bulk plasma, rather than sheath or presheath. The Debye length (0.1–1 mm) was small compared to the probe radius. Plasma potential profiles were measured using an emissive probe operated in the limit of zero emission, providing a spatial resolution of approximately 1 mm and a potential measurement error within ±0.5 V.[15]

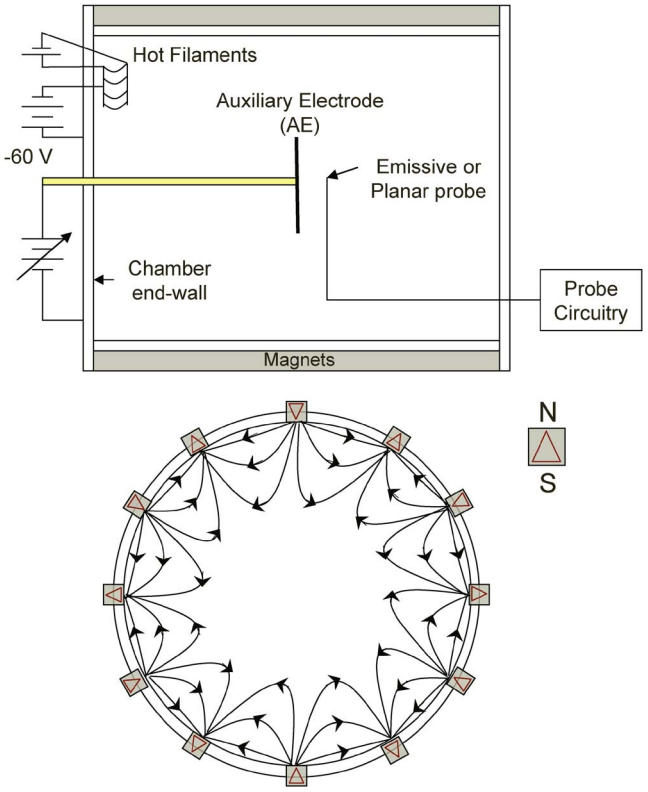

FIG. 1. (Color online) Experimental setup.

IV. EXPERIMENTAL RESULTS AND DISCUSSION

Figure 2 shows potential profiles for a monotonic ion sheath, a double sheath, and a monotonic electron sheath near AE of surface area 360, 150, and 20 cm^2, respectively. Data were taken at 0.7 mTorr neutral pressure. The total wall area available for particle loss included diffusion through the multidipole magnetic field, but the leak width for this loss depended on the plasma temperature and density. The plasma density was different in each case because the energy of filament electrons (which ionize neutrals) depended on the plasma potential and the electron temperature depended on the mode of plasma flow. If A_w was approximately the geometric area of the chamber end walls and half the geometric area of the chamber side wall, then $A_w \approx 18850$ cm^2. μ is 5.6×10^{-3} for an argon plasma, so Eqs. (4), (6), and (7) predict that for $A_{AE} > 180$ cm^2, the sheath near the AE should be a monotonic ion sheath, for $A_{AE} < 105$ cm^2 it should be a monotonic electron sheath, and for A_{AE} between these two values it should be a double sheath. The AE areas were chosen specifically to demonstrate each of these three sheath regimes. The detailed potential data of Fig. 2, which were taken with an emissive probe, show clearly each of the three predicted sheath structures. The 360 cm^2 AE features a monotonic ion sheath, the 20 cm^2 AE a monotonic electron sheath, and the 150 cm^2 AE a double sheath.

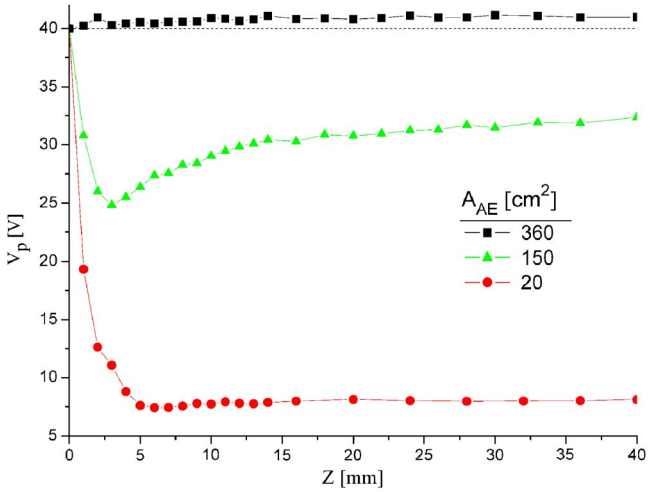

FIG. 2. (Color online) Potential profiles, in V, show a monotonic ion sheath (squares), a double sheath (triangles), and a monotonic electron sheath (circles) near AEs of 360, 150, and 20 cm^2, respectively. The dashed line illustrates for reference the 40 V AE bias. Data were taken at 0.7 mTorr neutral pressure.

Figure 3 shows the relationship between plasma potential and AE potential for the monotonic ion, double, and monotonic electron sheaths near AEs of area 360, 120, and 57 cm^2, respectively. Data were taken at 1.0 mTorr neutral pressure. Bulk plasma parameters are summarized in Table I for AE biases 0 and +40 V. Figure 3 demonstrates that for the electron and double sheath solutions, there is a region between 0 and 20 V where the sheath transitioned from a monotonic ion sheath to a double sheath or electron sheath. This is the region at which the bulk electron temperature makes the transition from its value for global ambipolar flow (typically ~0.6 eV) at negative AE biases to its value for global nonambipolar flow (typically 2–3 eV). For AE biases larger than 20 V, the plasma potential "locks" with the AE

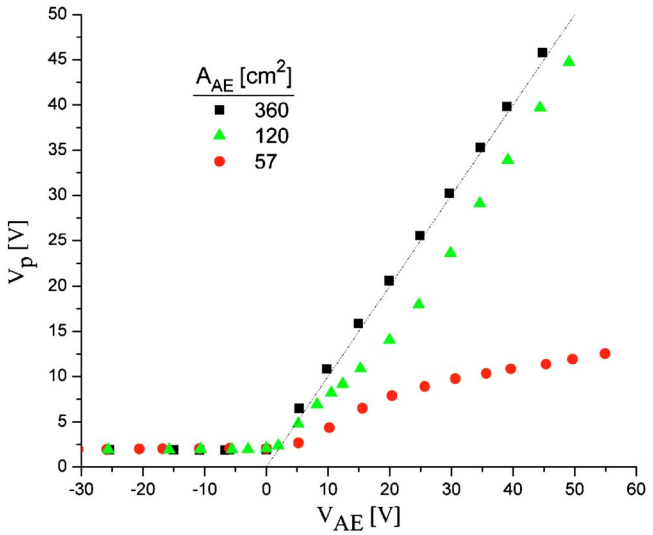

FIG. 3. (Color online) Plasma potential as a function of AE bias (in V) for AE areas of 360 cm^2 (squares), 120 cm^2 (triangles), and 57 cm^2 (circles) at 1.0 mTorr neutral pressure. The dashed line shows equal plasma and AE potential. Potentials were measured in the bulk plasma with a planar Langmuir probe.

TABLE I. Bulk plasma parameters measured with a planar Langmuir probe.

V_{AE} (V)	A_{AE} (cm^2)	T_e (eV)	V_p (V)	$I_{e,AE}$ (A)	n_e (10^9 cm^{-3})
0	57	0.7	2.0	0	2.1
0	120	0.6	2.0	0	1.7
0	360	0.6	1.9	0	1.3
40	57	2.2	11	0.31	0.9
40	120	2.4	34	0.53	1.5
40	360	1.5	41	0.71	1.6

potential in the double sheath case, suggesting that the potential drop of the dip remains fixed, as predicted by Eq. (8) and the argument following Eq. (9). The plasma potential remains nearly constant in the electron sheath case, as suggested by Eq. (5). The plasma potential always remains more positive than the largest AE, as Eq. (7) indicates, since an ion sheath solution is required. Although biasing this large AE biases the entire plasma, the bulk plasma remains quasineutral. If biasing the entire plasma were to cause a depletion in electron density, Boltzmann's relation, $n(x) = n_0 \exp(-e\Delta\varphi/T_e)$, would require a potential drop. Figure 2 shows that the only potential drops, or raises, are located in the sheaths and hence the plasma remains quasineutral. V_p does not rise due to a depletion in bulk electron density, it is simply the value for which the resulting boundary sheaths globally balance the electron and ion losses from the plasma.

An important feature of the double sheath that Fig. 3 illustrates is that the difference between the plasma potential and the AE potential was independent of AE bias for very positive values. This potential "locking" was utilized to establish global nonambipolar flow since the AE was used to raise the plasma potential to a magnitude that blocked all electrons from escaping the potential drop of the ion sheath at the chamber wall. All electrons were then lost only to the AE, while all ions were lost only to the chamber wall.

Table I shows that the electron temperature was largest when a double sheath was present, which is expected since this was the global nonambipolar flow regime. At 40 V, the ion sheath solution actually collected more net electron current than the double sheath. This occurred because the larger plasma potential produced more energetic filament electrons, resulting in a larger plasma density. Also, the larger plasma potential prevented energetic electrons originating at the filaments from being lost to the chamber wall, confining them to the plasma until they reached the AE. These high-energy electrons were injected by the hot filaments and therefore did not balance any corresponding ion current lost from the plasma. However, for large plasma potentials, filament electrons were also reflected from the chamber wall and subsequently lost to the AE. This effect is more clearly seen in Fig. 4.

Figure 4 shows planar probe data for the same 120 cm^2 AE as Fig. 3. When the double sheath formed (near 10 V), the net electron current collected by the AE was simply the incident thermal electron current calculated from the measured n_e and T_e. Since the plasma potential "locked" with the

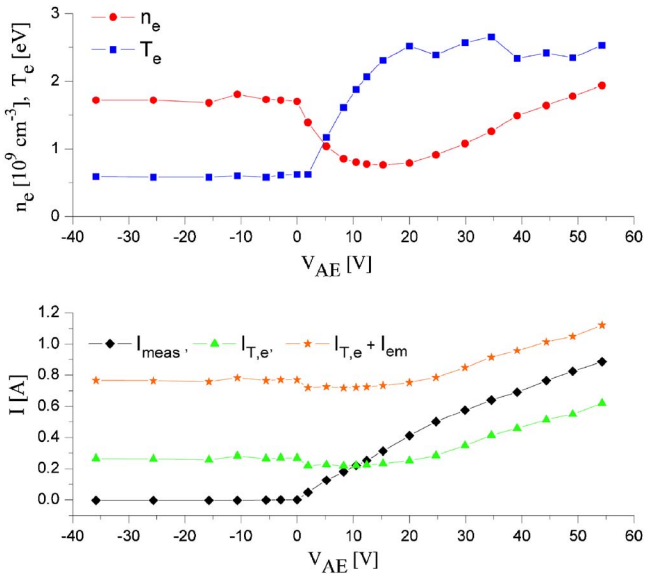

FIG. 4. (Color online) (Top) T_e(eV) (squares) and electron density $n_e(10^9\ \mathrm{cm}^{-3})$ (circles) in the bulk region for AE area 120 cm^2. (Bottom) Predicted thermal electron current incident of the AE sheath from measured T_e and n_e (triangles), the measured net electron current collected by the AE (diamonds), and the sum of the predicted thermal electron current and 0.5 A filament current (stars).

AE potential for this AE, increasing the AE bias further made the potential drop of the ion sheath larger at the chamber wall. Subsequently, more high-energy electrons, both from the filaments and the thermal plasma, were reflected from the chamber wall and eventually lost to the AE.

The region of Fig. 4 from 0–15 V AE bias shows the characteristic temperature increase for the transition from global ambipolar flow to global nonambipolar flow. For $V_{\mathrm{AE}}<0$ V, $V_p\approx 2$ V and high-energy electrons (with energy $>eV_p$) were lost to the big chamber wall, A_w. Low-energy electrons (with energy $<eV_p$) could not escape the plasma to any boundary due to confining ion sheaths at each boundary. This scenario is characteristic of global ambipolar flow. When $V_{\mathrm{AE}}>\sim 15$ V, Fig. 3 shows $V_p\approx V_{\mathrm{AE}}-5$ V, and high-energy electrons were lost only to the small AE of area A_{AE} instead of the large area A_w, resulting in better confinement of high-energy electrons. Low-energy electrons were lost to A_{AE}, whereas in global ambipolar flow they were entirely confined. The combination of increased confinement of high-energy electrons and decreased confinement of low-energy electrons produced the bulk electron temperature increase shown in Fig. 4.

Because the plasma potential "locked" with the AE potential for positive biases, an increased AE bias produced more energetic filament emitted electrons, which in turn ionized more neutrals. Filament electrons entered the plasma with an energy of approximately $e(V_p+60V)$. An increase in bulk plasma density corresponding to the increased plasma potential was measured for AE biases greater than ~20 V. This effect is shown in Fig. 4, where the corresponding plasma potentials are shown in Fig. 3. Electron density increased approximately linearly with V_p when the electron temperature was a constant value in the global nonambipolar flow mode. However, a decrease in electron density was measured in the transition from the two global flow modes.

The energy contained in the plasma was determined by the input power, the device geometry, and the magnetic field. In the transition region from 0 to 15 V, the input power of the filament electrons was only modestly increased due to a plasma potential increase of approximately 10 V, see Fig. 3. Since the energy contained in the plasma is proportional to the product of density and the temperature, and temperature increased from the global ambipolar flow value, ~0.6 eV, to the global nonambipolar flow value, ~2.4 eV, the bulk electron density declined. Figure 4 illustrates the decrease of electron density in the transition region of the mode of global flow. The electron density lost in this transition region was later regained when the AE potential, and hence V_p, were further raised and consequently raised the input power to the plasma by creating more energetic filament-emitted electrons. The only change in total plasma loss was due to changes in the input power via controlling the plasma potential with the AE bias. Figures 3 and 4 show that when the input power was increased, the bulk plasma density, n_0, and correspondingly the net electron current collected by the AE, increased. After global nonambipolar flow was established for $V_{\mathrm{AE}}\approx 15$ V, the increased electron current collected by the AE was due to the increase of input power via increased plasma potential and not from a change the global flow regime, which is global nonambipolar flow for $V_{\mathrm{AE}}>15$ V.

Data shown in Fig. 4 demonstrate the characteristics of global nonambipolar flow where, via control of the plasma potential, essentially all electrons, including both those born from ionization and those emitted from hot filaments, were collected by a single boundary that collected no positive ions. All positive ions were lost to a different boundary.

V. SUMMARY

We showed that Langmuir's suggestion that the presence of either an electron or an ion sheath near a positively biased electrode depends on the electrode surface area was basically correct, but that the situation is slightly more complicated. The sheath near a positive electrode can be either a monotonic ion sheath, a monotonic electron sheath, or a double sheath, and each solution depends on the electron collection area *as well as* the ion collection area. We established a necessary condition that the ratio of these surface areas must satisfy for each sheath solution. We showed that when a double sheath is present, global nonambipolar flow can be established where all electrons are lost to only one boundary while all positive ions are lost elsewhere. Global nonambipolar flow is entirely a sheath effect, so the bulk plasma remains quasineutral, and it is an efficient way to separate plasma electrons and ions. Global nonambipolar flow can also be used to heat the plasma electrons, relative to their temperature in ambipolar flow, by more effectively trapping those with high energy and less effectively trapping those with low energy.

ACKNOWLEDGMENTS

The authors are grateful for experimental assistance from Alan Hoskinson and Shi Luo Yan and for assistance in preparing the manuscript from Dr. Debra Hershkowitz. This work was supported by U.S. DOE Grant No. DE-FG02-97ER5447 and the Wisconsin Space Grant Consortium (B.L.).

[1] L. Tsendin, Sov. Phys. Tech. Phys. **31**, 169 (1986).
[2] F. G. Baksht, G. A. Dyvzhev, A. M. Martsinovskiy, B. Ya. Moyzhes, G. Ye. Pikus, E. B. Sonin, and V. G. Yur'yev, *Thermionic Convertors and Low-Temperature Plasma*, edited by L. K. Hansen (National Technical Information Service/U.S. Department of Energy, Springfield, 1978).
[3] J. F. Waymouth, *Electric Discharge Lamps* (MIT Press, Cambridge, 1971).
[4] K. Jameson, D. Goebel, I. Mikellides, and R. Watkins, Proceedings of the 42nd Joint Propulsion Conference and Exhibit, Sacramento, CA, 9–12 July 2006, Paper No. AIAA-2006-4490.
[5] H. Morgner, M. Neumann, S. Straach, and M. Krug, Surf. Coat. Technol. **109**, 513 (1998).
[6] A. Krokhmal, J. Z. Gleizer, Ya. E. Krasik, J. Felsteiner, and V. I. Gushenets, J. Appl. Phys. **94**, 44 (2006).
[7] A. Hellmich, T. Jung, A. Kielhorn, and M. Rissland, Surf. Coat. Technol. **98**, 1541 (1998).
[8] J. E. Foster and M. J. Patterson, J. Propul. Power **21**, 144 (2005).
[9] B. Longmier, S. Baalrud, and N. Hershkowitz, Rev. Sci. Instrum. **77**, 113504 (2006).
[10] I. Langmuir, Phys. Rev. **33**, 954 (1929).
[11] F. F. Chen, *Introduction to Plasma Physics and Controlled Fusion. Vol. 1: Plasma Physics* (Plenum, New York, 1984).
[12] D. Bohm, in *Characteristics of Electrical Discharges in Magnetic Fields*, edited by A. Guthrie and R. K. Wakerling (McGraw-Hill, New York 1949), Vol. 1, p. 77.
[13] R. Limpaecher and K. R. MacKenzie, Rev. Sci. Instrum. **44**, 726 (1973).
[14] X. Wang and N. Hershkowitz, Rev. Sci. Instrum. **77**, 043507 (2006).
[15] N. Hershkowitz, in *Plasma Diagnostics*, edited by O. Auciello and D. L. Flamm (Academic, Boston, 1989), Vol. 1, p. 113.